Quantum oscillations in electron-doped high-temperature superconductors

Jonghyoun Eun, Xun Jia, and Sudip Chakravarty
Department of Physics and Astronomy, University of California–Los Angeles, Los Angeles, California 90095-1547, USA
(Received 25 August 2010; published 23 September 2010)

Quantum oscillations in hole-doped high-temperature superconductors are difficult to understand within the prevailing views. An emerging idea is that of a putative normal ground state, which appears to be a Fermi liquid with a reconstructed Fermi surface. The oscillations are due to formation of Landau levels. Recently the same oscillations were found in the electron-doped cuprate, $Nd_{2-x}Ce_xCuO_4$, in the optimal to overdoped regime. Although these electron-doped nonstoichiometric materials are naturally more disordered, they strikingly complement the hole-doped cuprates. Here we provide an explanation of these observations from the perspective of density waves using a powerful transfer matrix method to compute the conductance as a function of the magnetic field.

DOI: 10.1103/PhysRevB.82.094515 PACS number(s): 74.72.Ek, 74.20.−z, 74.25.Ha, 74.25.Jb

I. INTRODUCTION

Periodically a class of experiments tend to disturb the status quo of the prevailing views in the area of high-temperature cuprate superconductors. Recent quantum oscillation (QO) experiments[1–8] fall into this category.[9] The first set of experiments were carried out in underdoped high-quality crystals of well-ordered $YBa_2Cu_3O_{6+\delta}$ (YBCO), stoichiometric $YBa_2Cu_4O_8$, and the overdoped single-layer $Tl_2Ba_2CuO_{6+\delta}$.[10]

More recently oscillations are also observed in electron-doped $Nd_{2-x}Ce_xCuO_4$ (NCCO).[11] The measurements in NCCO for 15%, 16%, and 17% doping[11] are spectacular. The salient features are: (1) the experiments are performed in the range 30–64 T, far above the upper critical field, which is about 10 T or less; (2) the material involves single CuO plane, and therefore complications involving chains, bilayers, Ortho-II potential,[12] etc., are absent; (3) stripes[13] may not be germane in this case.[14] It is true, however, that neither spin-density wave (SDW) nor *d*-density wave (DDW) (Ref. 15) are yet directly observed in NCCO in the relevant doping range but QOs seem to require their existence, at least the *field-induced* variety (see, however Ref. 16); (4) these experiments are a tour de force because the sample is nonstoichiometric with naturally greater intrinsic disorder. The effect is therefore no longer confined to a limited class of high-quality single crystals; (5) the authors have also succeeded in seeing the transition from low- to high-frequency oscillations[17] in NCCO as a function of doping.

Here we focus on NCCO. We shall see that disorder plays an important role. Without it is impossible to understand why the slow oscillations damp out below 30 T for 15% and 16% doping, and below 60 T for 17% doping, even though the field range is very high. For 17% doping, where a large hole pocket is observed corresponding to very fast oscillations (inconsistent with any kind of density wave order), the necessity of such high fields can have only one explanation, namely, to achieve a sufficiently large $\omega_c\tau$, where $\omega_c = eB/m^*c$, τ is the scattering lifetime of the putative normal phase, m^* the effective mass, and B the magnetic field. Qualitatively, the Dingle factor, D, that suppresses quantum oscillations is $D=e^{-p\pi/\omega_c\tau}$, where p is the index for the harmonic. Assuming a Fermi velocity, suitably averaged over an orbit to be v_F, the mean-free path $l=v_F\tau$. Thus D can be rewritten as $D=e^{-p\pi\hbar ck_F/eBl}$. A crude measure for k_F is given by expressing the area of an extremal orbit, A, as $A=\pi k_F^2$. By setting $m^*v_F=\hbar k_F$, the explicit dependence on the parameters m^* and v_F was eliminated. Assuming that the mean-free paths for the hole and the electron pockets are more or less the same, not an unreasonable assumption, the larger pockets, with larger k_F, will be strongly suppressed for the same value of the magnetic field because of the exponential sensitivity of D to the pocket size. This argument is consistent with our exact transfer matrix calculation using the Landauer formula for the conductance presented below.

Here we show that the oscillation experiments in NCCO reflect a broken translational symmetry[18] that reconstructs the Fermi surface in terms of electron and hole pockets.[9] The emphasis is not the transfer matrix method itself but its use in explaining a major experiment in some detail. We study both SDW and singlet DDW orders with the corresponding mean-field Hamiltonians. A more refined calculation, beyond the scope of the present paper, will be necessary to see the subtle distinction between the two order parameters.

In Sec. II, we introduce our mean-field Hamiltonians and in Sec. III, we discuss the transfer matrix method for the computation of quantum oscillations of the conductance. Section IV contains the results of our numerical computations and Sec. V our conclusions.

II. MEAN-FIELD HAMILTONIAN

We suggest that the experiments in NCCO can be understood from a suitable normal state because the applied magnetic fields between 30 and 65 T are so far above the upper critical field, which is less than 10 T, that vortex physics and the superconducting gap are not important. Our assumption is that a broken translational symmetry state with an ordering vector $\mathbf{Q}=(\pi/a,\pi/a)$ (a being the lattice spacing) can reconstruct the Fermi surface resulting in two hole pockets and one electron pocket within the reduced Brillouin zone, bounded by the constraints on the wave vectors $k_x \pm k_y = \pm \pi/a$. One challenge here is to understand why the large electron pockets corresponding to 15% and 16% doping re-

TABLE I. The band parameters, the chemical potential, and the mean-field parameters for DDW and SDW used in our calculation. F in tesla corresponds to the calculated oscillation frequencies of the hole pocket, the so-called slow frequencies. The measured F for 15% doping is 290 ± 10 T and for 16% doping is 280 ± 15 T. The calculated magnitude of F does depend on the neglected t''.

Order	t (eV)	t'	W_0	V_S	μ	V_0	F (T)
DDW 15%	0.3	$0.45t$	$0.1t$	*	$-0.40t$	$0.8t$	195
DDW 16%	0.3	$0.45t$	$0.1t$	*	$-0.365t$	$0.8t$	165
SDW 15%	0.3	$0.45t$	*	$0.05t$	$-0.403t$	$0.8t$	195
SDW 16%	0.3	$0.45t$	*	$0.05t$	$-0.366t$	$0.8t$	173

sulting from the band-structure parameters for NCCO defined below are not observed but the much smaller hole pockets are. Another challenge is to understand why the large Fermi surface at 17% doping is not observed until the applied field reaches about 60 T. The reason we believe is the existence strong cation disorder in this material. It is therefore essential to incorporate disorder in our Hamiltonian. For the Hamiltonian itself, we consider a mean-field approach, and for this purpose we consider two possible symmetries, one that corresponds to a singlet in the spin space (DDW) and one that is a triplet in the spin space (SDW). Note that these are particle-hole condensates for which orbital function does not constrain the spin wave function unlike a particle-particle condensate (superconductor) because there are no exchange requirements between a particle and a hole.

We believe that it is reasonable that as long as a system is deep inside a broken symmetry state, mean-field theory and its associated elementary excitations should correctly capture the physics. The fluctuation effects will be important close to quantum phase transitions. However, there are no indications in the present experiments that fluctuations are important. The microscopic basis for singlet DDW Hamiltonian is discussed in some detail in Refs. 19 and 20, and in references therein. So, we do not see any particular need to duplicate this discussion here. The mean-field Hamiltonian for the singlet DDW in real space, in terms of the site-based fermion annihilation and creation operators of spin σ, $c_{\mathbf{i},\sigma}$, and $c^{\dagger}_{\mathbf{i},\sigma}$, is

$$H_{\mathrm{DDW}} = \sum_{\mathbf{i},\sigma} \epsilon_{\mathbf{i}} c^{\dagger}_{\mathbf{i},\sigma} c_{\mathbf{i},\sigma} + \sum_{\mathbf{i},\mathbf{j},\sigma} t_{\mathbf{i},\mathbf{j}} e^{ia_{\mathbf{i},\mathbf{j}}} c^{\dagger}_{\mathbf{i},\sigma} c_{\mathbf{j},\sigma} + \mathrm{H.c.}, \tag{1}$$

where the nearest-neighbor hopping matrix elements are

$$t_{\mathbf{i},\mathbf{i}+\hat{\mathbf{x}}} = -t + \frac{iW_0}{4}(-1)^{(\mathbf{i}_x+\mathbf{i}_y)}, \tag{2}$$

$$t_{\mathbf{i},\mathbf{i}+\hat{\mathbf{y}}} = -t - \frac{iW_0}{4}(-1)^{(\mathbf{i}_x+\mathbf{i}_y)}. \tag{3}$$

Here W_0 is the DDW gap. We also include the next-nearest-neighbor hopping t' whereas the third-neighbor hopping t'' is ignored to simplify computational complexity without losing the essential aspects of the problem. The parameters t and t' are chosen (see Table I) to closely approximate the more conventional band structure, as shown in Fig. 1. We have checked that the choice $t''=0$ provides reasonably consistent results for the frequencies in the absence of disorder. For example, for DDW, and 15% doping, the hole pocket frequency is 185 T, and the corresponding electron pocket frequency is 2394 T.

Similarly, the SDW mean-field Hamiltonian is

$$H_{\mathrm{SDW}} = \sum_{\mathbf{i},\sigma} [\epsilon_{\mathbf{i}} + \sigma V_S (-1)^{\mathbf{i}_x+\mathbf{i}_y}] c^{\dagger}_{\mathbf{i},\sigma} c_{\mathbf{i},\sigma} + \sum_{\mathbf{i},\mathbf{j},\sigma} t_{\mathbf{i},\mathbf{j}} e^{ia_{\mathbf{i},\mathbf{j}}} c^{\dagger}_{\mathbf{i},\sigma} c_{\mathbf{j},\sigma} + \mathrm{H.c.} \tag{4}$$

and the spin $\sigma = \pm 1$ while the magnitude of the SDW amplitude is V_S. In both cases, a constant perpendicular magnetic field B is included via the Peierls phase factor $a_{\mathbf{i},\mathbf{j}} = \frac{2\pi e}{h} \int_{\mathbf{j}}^{\mathbf{i}} \mathbf{A} \cdot d\mathbf{l}$, where $\mathbf{A} = (0, -Bx, 0)$ is the vector potential in the Landau gauge. We note that usually a perpendicular magnetic field, even as large as 60 T, has little effect on the DDW gap,[21] except close to the doping at which it collapses, where field-induced order may be important.

We have seen previously[19] that the effect of long-ranged correlated disorder is qualitatively similar to white noise insofar as the QOs are concerned. The effect of the nature of

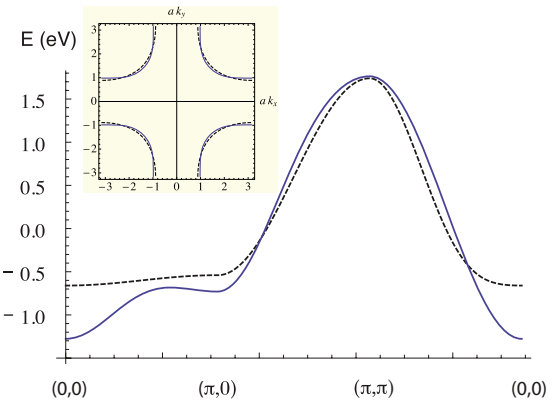

FIG. 1. (Color online) The solid curve represents the t-t'-t'' band structure ($t=0.38$ eV, $t'=0.32t$, $t''=0.5t'$), and the dashed curve corresponds to t-t' band structure, (see Table I). The quasiparticle energy is plotted in the Brillouin zone along the triangle $(0,0) \rightarrow (\pi,0) \rightarrow (\pi,\pi) \rightarrow (0,0)$. In the inset, the chemical potential, μ, was adjusted to obtain approximately 15% doping.

disorder on the spectral function of angle-resolved photoemission spectroscopy (ARPES) was found to be far more important. The reason is that the coherence factors of the ARPES spectral function are sensitive to the nature of the disorder because they play a role similar to Wannier functions. In contrast, the QOs are damped by the Dingle factor, which is parametrized by a single lifetime and disorder enters in an averaged sense.

Thus, it is sufficient to consider on-site disorder. The on-site energy is δ-correlated white noise defined by the disorder average $\overline{\epsilon_i}=0$ and $\overline{\epsilon_i \epsilon_j}=V_0^2 \delta_{i,j}$. For an explicit calculation, we need to choose the band-structure parameters, W_0, V_S, and the disorder magnitude V_0. When considering the magnitude of disorder one should keep in mind that the full bandwidth is $8t$. The magnetic field ranges roughly between 30 and 64 T, representative of the experiments in NCCO. The magnetic length is $l_B=\sqrt{\hbar/eB}$, which for $B=30$ T is approximately $12a$, where the lattice constant a is equal to 3.95 Å.

The effect of potential scattering that modulates charge density is indirect on twofold commensurate SDW or DDW order parameter,[22] mainly because SDW is modulation of spin and DDW that of charge current. Thus, the robustness of these order parameters with respect to disorder protects the corresponding quasiparticle excitations insofar as quantum oscillations are concerned, as seen below in our exact numerical calculations. Thus we did not find it important to study this problem self consistently.

III. TRANSFER MATRIX METHOD

The transfer matrix method and the calculation of the Lyapunov exponents sketched elsewhere[19] is fully described here for the case of singlet DDW; for SDW the generalization is straightforward, where the diagonal term must be modified because of V_S, and the term W_0 will be absent. Consider a quasi-one-dimensional system, $L \gg M$, with a periodic boundary condition along y direction. Let $\Psi_n=(\psi_{n,1},\psi_{n,2},\ldots,\psi_{n,M})^T$ be the amplitudes on the slice n for an eigenstate with a given energy, then the amplitudes on three successive slices satisfy the relation

$$\begin{bmatrix} \Psi_{n+1} \\ \Psi_n \end{bmatrix} = \begin{bmatrix} T_n^{-1}A_n & -T_n^{-1}B_n \\ 1 & 0 \end{bmatrix} \begin{bmatrix} \Psi_n \\ \Psi_{n-1} \end{bmatrix} = \mathbf{T}_n \begin{bmatrix} \Psi_n \\ \Psi_{n-1} \end{bmatrix}, \tag{5}$$

where T_n, A_n, and B_n are $M \times M$ matrices. The nonzero matrix elements of the matrix A_n are

$$(A_n)_{m,m} = \epsilon_{n,m} - \mu,$$

$$(A_n)_{m,m+1} = \left[-t + \frac{iW_0}{4}(-1)^{m+n} \right] e^{-in\phi},$$

$$(A_n)_{m,m-1} = \left[-t + \frac{iW_0}{4}(-1)^{m+n} \right] e^{in\phi}, \tag{6}$$

where $\phi=2\pi B a^2 e/h$ is a constant. For the matrix B_n,

$$(B_n)_{m,m} = -\left[-t - \frac{iW_0}{4}(-1)^{m+n} \right],$$

$$(B_n)_{m,m+1} = -t' e^{i(-n+1/2)\phi},$$

$$(B_n)_{m,m-1} = -t' e^{i(n-1/2)\phi}. \tag{7}$$

For the matrix T_n, we note that $T_n=B_{n+1}^{\dagger}$.

The $2M$ Lyapunov exponents, γ_i, of $\lim_{N\to\infty}(\mathcal{T}_N\mathcal{T}_N^{\dagger})^{1/2N}$, where $\mathcal{T}_N=\Pi_{j=1}^{j=N}\mathbf{T}_j$, are defined by the corresponding eigenvalues $\lambda_i=e^{\gamma_i}$. All Lyapunov exponents $\gamma_1>\gamma_2>\ldots>\gamma_{2M}$, are computed by a procedure given in Ref. 23. The modification here is that this matrix is not symplectic. Therefore all $2M$ eigenvalues have to be computed. The remarkable fact, however, is that except for a small fraction, consisting of larger eigenvalues, the rest do come in pairs $(\lambda, 1/\lambda)$, as for the symplectic case, within numerical accuracy. We have no analytical proof of this curious fact. Clearly, larger eigenvalues contribute insignificantly to the more general formula for the conductance,[24]

$$\sigma(B) = \frac{e^2}{h} \mathrm{Tr} \sum_{j=1}^{2M} \frac{2}{(\mathcal{T}_N\mathcal{T}_N^{\dagger}) + (\mathcal{T}_N\mathcal{T}_N^{\dagger})^{-1} + 2}. \tag{8}$$

When the eigenvalues do come in pairs, the conductance formula simplifies to the more common Landauer formula,[25]

$$\sigma_{xx}(B) = \frac{e^2}{h} \sum_{i=1}^{M} \frac{1}{\cosh^2(M\gamma_i)}. \tag{9}$$

The transfer matrix method is a very powerful method and the results obtained are rigorous compared to *ad hoc* broadening of the Landau levels, which also require more adjustable parameters to explain the experiments. Once the distribution of disorder is specified there are no further approximations. We note that the values of M were chosen to be much larger than our previous work,[19] at least 128 (that is, 128 a in physical units) and sometimes as large as 512. The length of the strip L is varied between 10^5 and 10^6. This easily led to an accuracy better than 5% for the smallest Lyapunov exponent, γ_i, in all cases.

We have calculated the ab-plane conductance but the measured c-axis resistance, R_c, is precisely related to it, at least as far as the oscillatory part is concerned. This can be seen from the arguments in Ref. 26. Although the details can be improved, the crux of the argument is that the planar density of states enters R_c: the quasiparticle scatters many times in the plane while performing cyclotron motion before hopping from plane to plane (measured ab-plane resistivity is of the order 10 $\mu\Omega$ cm as compared to 1 Ω cm for the c-axis resistivity even at optimum doping[14]). It is worth noting that oscillations of R_c also precisely follows the oscillations of the magnetization in overdoped $Tl_2Ba_2CuO_{6+\delta}$.[10]

IV. RESULTS

There are clues in the experiments[11] that disorder is very important. For 15% and 16% doping, the slow oscillations in experiments, of frequency 290–280 T, are not observed until the field reaches above 30 T, which is much greater than $H_{c2}<10$ T. For 17% doping the onset of fast oscillations at a frequency of 10,700 T are strikingly not observable until

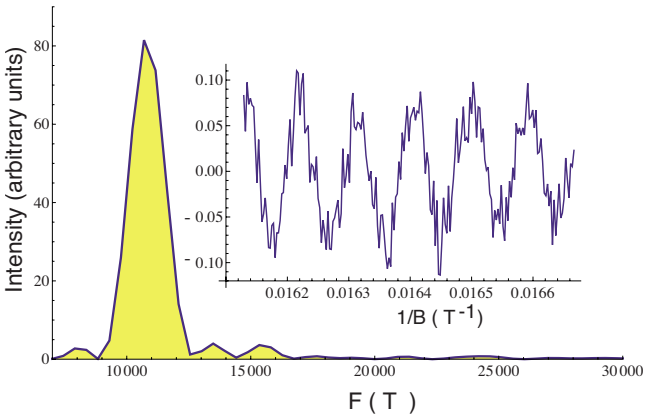

FIG. 2. (Color online) The main plot shows the Fourier transform of the field sweep shown in the inset. The peak is at 10 695 T. The inset is a smooth background subtracted Shubnikov de Haas oscillations, as calculated from the Landauer formula for 17% doping as a function of $1/B$. The disorder parameter is $V_0=0.7t$. The band-structure parameters are given in Table I.

the field reaches 60 T. The estimated scattering time from the Dingle factor at even optimal doping and at 4 K is quite short.

For 17% doping corresponding to $\mu=-0.322t$ and the band structure given in Table I, a slight change in disorder from $V_0=0.7t$ to $V_0=0.8t$ makes the difference between a clear observation of a peak to simply noise within the field sweep between 60 and 62 T, as shown in Figs. 2 and 3. Since in this case $W_0=V_S=0$, there is little else to blame for the disappearance of the oscillations for fields roughly below 60 T. The results are essentially identical for small values of W_0, such as $0.025t$.

For 15% and 16% dopings, we chose V_0 to simulate the fact that oscillations seem to disappear below 30 T. The field sweep was between 30 and 60 T. The results for DDW order are shown in Figs. 4 and 5.

The most remarkable feature of these figures is that disorder has completely wiped out the large electron pocket leaving the small hole pocket visible. To emphasize this

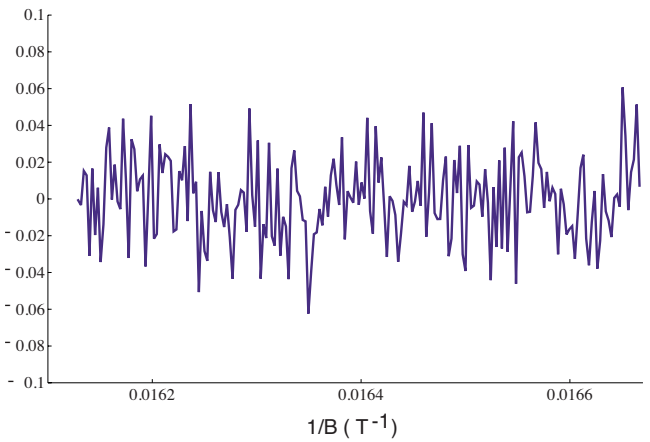

FIG. 3. (Color online) The same parameters as in Fig. 2 but $V_0=0.8t$. The background subtracted conductance is simply noise to an excellent approximation.

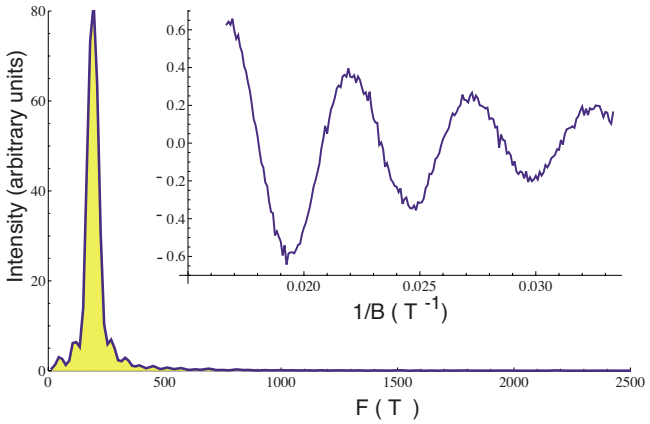

FIG. 4. (Color online) The same plot as in Fig. 2, except for 15% doping and DDW order. The parameters are given in Table I.

point, we also plot the results for 15% doping but with much smaller disorder $V_0=0.2t$; see Fig. 6. Now we can see the fragmented remnants of the electron pocket. With further lowering of disorder, the full electron pocket becomes visible. It is clear that disorder has a significantly stronger effect on the electron pockets than on the hole pockets. This, as we noted earlier, is largely due to higher density of states around the antinodal points, which significantly accentuates the effect of disorder.[19]

We have done parallel calculations with SDW order as well. The results are essentially identical. They are shown again for 15% and 16% doping in Figs. 7 and 8. We have kept all parameters fixed while adjusting the SDW gap to achieve as best an approximation to experiments as possible.

It is important to summarize our results in the context of experimental observations. First, we were able to show that the electron pocket frequencies are strikingly absent because of disorder and the slow frequencies corresponding to the hole pocket for 15% and 16% doping damp out below about 30 T, even though H_{c2} is less than 10 T. Similarly, that the high-frequency oscillations at 17% doping do not arise until about 60 T has a natural explanation in terms of disorder, although in this case some magnetic breakdown effect, which was not explored, can be expected. This requires both

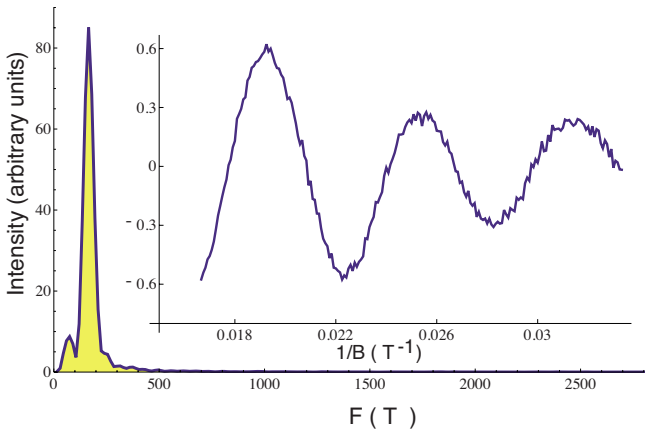

FIG. 5. (Color online) The same plot as in Fig. 2, except for 16% doping and DDW order. The parameters are given in Table I.

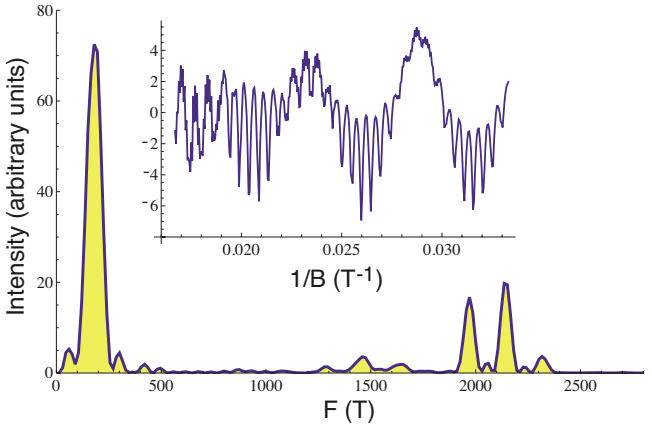

FIG. 6. (Color online) The same plot as in Fig. 4, except that $V_0=0.2t$ instead of $0.8t$. There is now a fragmented electron pocket centered around 2100 T and the main peak is at 183 T. The rest of the parameters are given in Table I.

further experimental and theoretical investigations. The calculated frequency of the high-frequency oscillations, 10 695 T is remarkably close to experimental value of 10, 700 ± 400 T. As to the magnitude of the slow oscillations, the calculated values are given in Table I, which are reasonable in both magnitude and trend when compared to experiments. The small discrepancies in the magnitude of F are due to our neglect of t'' in the band structure. This can be, and was, checked by checking the pure case, that is, without disorder.

V. CONCLUSIONS

In the absence of disorder or thermal broadening, the oscillation waveforms are never sinusoidal in two dimensions and contain many Fourier harmonics. At zero temperature, moderate disorder converts the oscillations to sinusoidal waveform with rapidly decreasing amplitudes of the harmonics. Further increase in disorder ultimately destroys the amplitudes altogether. Many experiments exhibit roughly sinusoidal waveform at even ultralow temperatures, implying

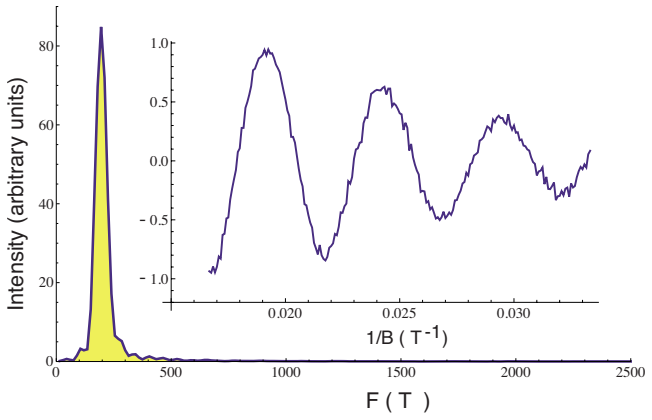

FIG. 7. (Color online) The same plot as in Fig. 4 for 15% doping but using SDW order. The main peak is at 195 T. The rest of the parameters are given in Table I.

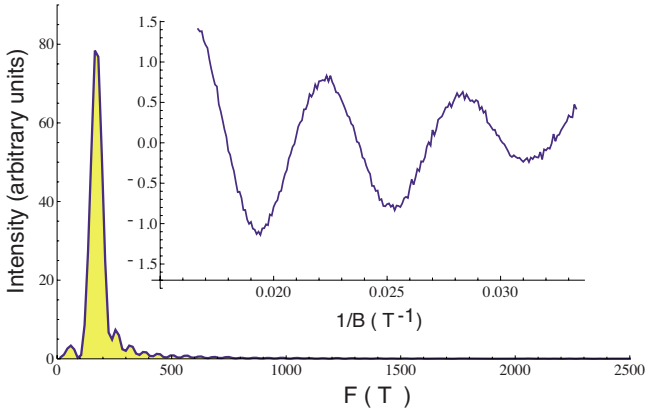

FIG. 8. (Color online) The same plot as in Fig. 7, except for 16% doping and using SDW order. The main peak is at 173 T. The rest of the parameters are given in Table I.

that disorder is important. The remarkably small electronic dispersion in the direction perpendicular to the CuO planes cannot alone account for the waveform.

For NCCO it is no longer a mystery as to why the frequency corresponding to the larger electron pocket is not observed. As we have shown, disorder is the culprit. Neither is the comparison with ARPES controversial,[14] as in the case of YBCO, since there is good evidence of Fermi-surface crossing in the direction $(\pi,0)\rightarrow(\pi,\pi)$, which is a signature of the electron pocket. The crossing along $(\pi,\pi)\rightarrow(0,0)$ can be easily construed as an evidence of a small hole pocket for which half of it is made invisible both from the coherence factors and disorder effects.[19] For electron-doped materials, such as NCCO and PCCO, it is known[14] that the Hall coefficient changes sign around 17% doping and therefore the picture of reconnection of the Fermi pockets is entirely plausible, with some likely magnetic breakdown effects. The real question is what is the evidence of SDW or DDW in the relevant doping range between 15% and 17%. From neutron measurements, we know that there is no long-range SDW order for doping above 13.4%.[27] We cannot rule out field-induced SDW at about 30 T. For DDW, there are no corresponding neutron measurements to observe its existence. Given that DDW is considerably more hidden[15,28] from common experiments, it is more challenging to establish it directly. NMR experiments in high fields for suitable nuclei can shed light on this question. The unavoidable logical conclusion from the QO measurements is that a density wave that breaks translational symmetry must be present. We suggest that motivated future experiments will be necessary to reach a definitive conclusion. Finally, at the level of mean-field theory we have been unable to decide between SDW and singlet DDW. At the moment the best recourse is to experimentally look for spin zeros in the amplitude of quantum oscillations in a tilted magnetic field. A theoretical discussion of this phenomenon that can potentially shed light between a triplet order parameter (SDW) and a singlet order parameter, the singlet DDW discussed here, was provided recently.[29] So far experiments are in conflict with each other in YBCO: one group suggests a triplet order parameter[30,31] and the other a singlet order parameter.[32]

It is unquestionable that the QO experiments are likely to change the widespread views in the field of high-temperature

superconductivity. Although the measurements in YBCO are not fully explained, the measurements in NCCO appear to have a clear and simple explanation, as shown here. However, given the similarity of the phenomenon in both hole- and electron-doped cuprates, it is likely that the quantum oscillations have the same origin.

ACKNOWLEDGMENTS

This work is supported by NSF under the Grant No. DMR-0705092. All calculations were performed at Hoffman 2 Cluster at UCLA. We thank E. Abrahams for a critical reading of the manuscript and N. P. Armitage for comments.

[1] N. Doiron-Leyraud, C. Proust, D. LeBoeuf, J. Levallois, J.-B. Bonnemaison, R. Liang, D. A. Bonn, W. N. Hardy, and L. Taillefer, Nature (London) **447**, 565 (2007).
[2] A. F. Bangura *et al.*, Phys. Rev. Lett. **100**, 047004 (2008).
[3] D. LeBoeuf *et al.*, Nature (London) **450**, 533 (2007).
[4] C. Jaudet *et al.*, Phys. Rev. Lett. **100**, 187005 (2008).
[5] E. A. Yelland, J. Singleton, C. H. Mielke, N. Harrison, F. F. Balakirev, B. Dabrowski, and J. R. Cooper, Phys. Rev. Lett. **100**, 047003 (2008).
[6] S. E. Sebastian, N. Harrison, E. Palm, T. P. Murphy, C. H. Mielke, R. Liang, D. A. Bonn, W. N. Hardy, and G. G. Lonzarich, Nature (London) **454**, 200 (2008).
[7] A. Audouard, C. Jaudet, D. Vignolles, R. Liang, D. A. Bonn, W. N. Hardy, L. Taillefer, and C. Proust, Phys. Rev. Lett. **103**, 157003 (2009).
[8] J. Singleton *et al.*, Phys. Rev. Lett. **104**, 086403 (2010).
[9] S. Chakravarty, Science **319**, 735 (2008).
[10] B. Vignolle, A. Carrington, R. A. Cooper, M. M. J. French, A. P. Mackenzie, C. Jaudet, D. Vignolles, C. Proust, and N. E. Hussey, Nature (London) **455**, 952 (2008).
[11] T. Helm, M. V. Kartsovnik, M. Bartkowiak, N. Bittner, M. Lambacher, A. Erb, J. Wosnitza, and R. Gross, Phys. Rev. Lett. **103**, 157002 (2009).
[12] D. Podolsky and H.-Y. Kee, Phys. Rev. B **78**, 224516 (2008).
[13] A. J. Millis and M. R. Norman, Phys. Rev. B **76**, 220503 (2007).
[14] N. Armitage, P. Fournier, and R. Green, Rev. Mod. Phys. **82**, 2421 (2010).
[15] S. Chakravarty, R. B. Laughlin, D. K. Morr, and C. Nayak, Phys. Rev. B **63**, 094503 (2001).
[16] P. Rourke, A. Bangura, C. Proust, J. Levallois, N. Doiron-Leyraud, D. LeBoeuf, L. Taillefer, S. Adachi, M. Sutherland, and N. Hussey, Phys. Rev. B **82**, 020514(R) (2010).
[17] C. Kusko, R. S. Markiewicz, M. Lindroos, and A. Bansil, Phys. Rev. B **66**, 140513 (2002).
[18] S. Chakravarty and H.-Y. Kee, Proc. Natl. Acad. Sci. U.S.A. **105**, 8835 (2008).
[19] X. Jia, P. Goswami, and S. Chakravarty, Phys. Rev. B **80**, 134503 (2009).
[20] I. Dimov, P. Goswami, X. Jia, and S. Chakravarty, Phys. Rev. B **78**, 134529 (2008).
[21] H. K. Nguyen and S. Chakravarty, Phys. Rev. B **65**, 180519 (2002).
[22] A. Ghosal and H.-Y. Kee, Phys. Rev. B **69**, 224513 (2004).
[23] B. Kramer and M. Schreiber, in *Computational Physics*, edited by K. H. Hoffmann and M. Schreiber (Springer, Berlin, 1996), p. 166.
[24] J. L. Pichard and G. André, Europhys. Lett. **2**, 477 (1986).
[25] D. S. Fisher and P. A. Lee, Phys. Rev. B **23**, 6851 (1981).
[26] N. Kumar and A. M. Jayannavar, Phys. Rev. B **45**, 5001 (1992).
[27] E. M. Motoyama, G. Yu, I. M. Vishik, O. P. Vajk, P. K. Mang, and M. Greven, Nature (London) **445**, 186 (2007).
[28] C. Nayak, Phys. Rev. B **62**, 4880 (2000).
[29] D. Garcia-Aldea and S. Chakravarty, arXiv:1008.2030 (unpublished).
[30] S. E. Sebastian, N. Harrison, C. H. Mielke, R. Liang, D. A. Bonn, W. N. Hardy, and G. G. Lonzarich, Phys. Rev. Lett. **103**, 256405 (2009).
[31] S. E. Sebastian, N. Harrison, P. A. Goddard, M. M. Altarawneh, C. H. Mielke, R. Liang, D. A. Bonn, W. N. Hardy, O. K. Andersen, and G. G. Lonzarich, Phys. Rev. B **81**, 214524 (2010).
[32] B. Ramshaw, B. Vignolle, J. Day, R. Liang, W. Hardy, C. Proust, and D. Bonn, arXiv:1004.0260 (unpublished).